nature structural & molecular biology

Translational control of the cytosolic stress response by mitochondrial ribosomal protein L18

Xingqian Zhang[1], Xiangwei Gao[1,4], Ryan Alex Coots[1,2], Crystal S Conn[3], Botao Liu[3] & Shu-Bing Qian[1–3]

In response to stress, cells attenuate global protein synthesis but permit efficient translation of mRNAs encoding heat-shock proteins (HSPs). Although decades have passed since the first description of the heat-shock response, how cells achieve translational control of HSP synthesis remains enigmatic. Here we report an unexpected role for mitochondrial ribosomal protein L18 (MRPL18) in the mammalian cytosolic stress response. MRPL18 bears a downstream CUG start codon and generates a cytosolic isoform in a stress-dependent manner. Cytosolic MRPL18 incorporates into the 80S ribosome and facilitates ribosome engagement on mRNAs selected for translation during stress. MRPL18 knockdown has minimal effects on mitochondrial function but substantially dampens cytosolic HSP expression at the level of translation. Our results uncover a hitherto-uncharacterized stress-adaptation mechanism in mammalian cells, which involves formation of a 'hybrid' ribosome responsible for translational regulation during the cytosolic stress response.

Cell survival in a changing environment requires swift regulation of gene expression, including translational control of existing mRNAs[1]. Global translation is generally suppressed in response to most, if not all, types of cellular stress[2,3]. However, subsets of transcripts undergo selective translation to produce proteins that are vital for cell survival and stress recovery. One of the best-known examples is the heat-shock protein 70 (Hsp70), whose synthesis is upregulated in cells upon elevated temperatures or exposure to proteotoxic stress[4,5]. Although transcriptional regulation after heat shock is well characterized[6,7], understanding of how efficient synthesis of HSPs persists when the translation machinery is generally compromised has remained elusive. It is commonly believed that the 5′ untranslated region (5′ UTR) of Hsp70 mRNA recruits the translational apparatus in a cap-independent manner[8–11]. However, neither the specific translation-promoting features of Hsp70 mRNAs nor the regulatory mechanism of the translation machinery has been clearly defined. In particular, it is unknown whether specialized ribosomes are required for efficient Hsp70 synthesis under stress conditions.

The ribosome is a large ribonucleoprotein complex composed of two subunits that associate upon the initiation of translation[12]. The small subunit decodes mRNA, and the large subunit catalyzes peptide-bond formation. In mammalian cells, there are two sets of ribosome particles, which reside in the cytoplasm and the mitochondria. Although ribosomal proteins (RPs) are all synthesized in the cytoplasm, they assemble into functional subunits in different subcellular compartments[13]. The mitochondrial RPs (MRPs) are encoded by nuclear genes, are synthesized in the cytosol and are then imported into mitochondria for assembly; they are responsible for translation of 13 mitochondrial mRNAs[14]. In contrast, cytosolic ribosomes are assembled within the nucleolus and are then exported into the cytoplasm for mRNA translation. Because of their distinct composition and cellular localization, there is believed to be little functional connection between mitochondrial and cytosolic ribosomes.

Here we set out to investigate whether specialized ribosomes are required in the cytosolic stress response. We report that MRPL18 bears a hidden CUG start codon downstream of the main initiation site. Stress conditions such as heat shock trigger CUG-initiated alternative translation, to generate a cytosolic isoform of MRPL18. We found that the cytosolic MRPL18 integrates into the 80S ribosome complex in a stress-dependent manner and facilitates synthesis of stress proteins such as Hsp70. Our results uncover a hitherto-uncharacterized stress-adaptation mechanism in mammalian cells, which involves formation of a hybrid ribosome that promotes synthesis of stress proteins.

RESULTS

MRPL18 alternative translation produces a cytosolic isoform

We used our previously developed approach, global translation initiation sequencing (GTI-seq), which allows precise mapping of alternative translation initiation sites (TISs) across the entire transcriptome[15]. The transcript encoding MRPL18 bears several interesting features. First, MRPL18 shows three TISs, with the annotated start codon (aTIS) flanked by an upstream TIS (uTIS) and a downstream TIS (dTIS) (**Fig. 1a**). Whereas the uTIS codon is an AUG, the dTIS uses CUG as the initiator. Intriguingly, the CUG initiator is located immediately after the predicted mitochondrial targeting signal (MTS) of MRPL18 and within the same reading frame. It is likely that CUG-initiated translation produces a cytosolic isoform of MRPL18. However, the identical size of cytosolic MRPL18 (MRPL18(cyto))

[1]Division of Nutritional Sciences, Cornell University, Ithaca, New York, USA. [2]Graduate Field of Nutritional Sciences, Cornell University, Ithaca, New York, USA. [3]Graduate Field of Genetics, Genomics and Development, Cornell University, Ithaca, New York, USA. [4]Present address: Institute of Environmental Medicine, Zhejinag University School of Medicine, Hangzhou, People's Republic of China. Correspondence should be addressed to S.-B.Q. (sq38@cornell.edu).

Received 21 November 2014; accepted 13 March 2015; published online 13 April 2015; doi:10.1038/nsmb.3010

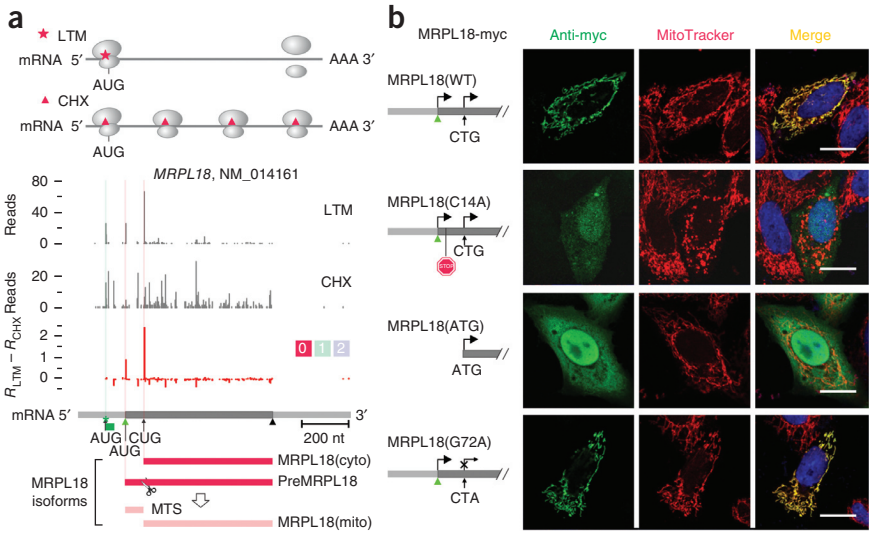

Figure 1 MRPL18 undergoes alternative translation to produce a cytosolic isoform. (**a**) Top, schematic of GTI-seq with translation inhibitors lactimidomycin (LTM) and cycloheximide (CHX). Raw read counts per nucleotide position of *MRPL18* are plotted as a bar graph. Middle, processed LTM read density (*R*), color-coded by the corresponding reading frame, with the identified TIS positions marked by asterisks. Bottom, predicted isoforms of MRPL18. (**b**) Immunostaining of HeLa cells transfected with MRPL18 wild type and mutants illustrated at left. Anti-myc is shown in the green channel and MitoTracker in the red channel. 4′,6-diamidino-2-phenylindole (DAPI) was used for nuclear counterstaining. Scale bars, 10 μm.

and the MTS-cleaved mitochondrial MRPL18 (MRPL18(mito)) renders them indistinguishable by standard immunoblotting.

To experimentally confirm the alternative translation of MRPL18, we constructed a series of MRPL18 mutants bearing myc tags and examined their subcellular localization in HeLa cells. The wild-type MRPL18 was mostly localized in mitochondria, as revealed by immunofluorescence staining (**Fig. 1b**). The vague cytoplasmic staining suggests that the CUG-initiated MRPL18(cyto) was not a major product under the normal growth condition. To show exclusively the CUG-initiated translation, we created a stop codon between the aTIS and the dTIS to prevent the synthesis of full-length MRPL18. This mutant, MRPL18(C14A), exhibited a clear localization in the cytosol and the nucleus (**Fig. 1b**). We saw a similar pattern for MRPL18(ATG), a truncated version of MRPL18 lacking both the 5′ UTR and the MTS. In contrast, MRPL18(G72A), a mutant with the dTIS mutated to CTA, showed a predominant mitochondrial localization. Together, these results indicate that MRPL18 bears a hidden downstream CUG start codon whose initiation gives rise to a cytosolic isoform of MRPL18.

MRPL18 undergoes stress-induced alternative translation

Notably, the CUG-only MRPL18(C14A) had much lower expression levels than other transgenes (**Fig. 1b** and **Supplementary Fig. 1a**), a result suggesting that the downstream CUG initiator is less efficient than the authentic AUG start codon. Interestingly, *Mrpl18* is a heat shock–responsive gene[16], and a recent study indicated that *MRPL18* is one of the direct targets of heat-shock transcription factor 1 (HSF1)[17]. Using a mouse fibroblast cell line lacking HSF1 (ref. 18), we confirmed the transcriptional upregulation of *Mrpl18* upon heat shock (**Supplementary Fig. 1b**). To investigate whether MRPL18 undergoes translational regulation in response to stress, we compared the abundance of transfected MRPL18 mutants in HeLa cells before and after heat shock. These transgenes maintained similar mRNA levels in response to heat shock (**Supplementary Fig. 1c**), thus allowing direct evaluation of translational control. Immunoblotting showed two bands of transfected MRPL18, corresponding to the MRPL18 precursor and the MRPL18 species lacking the MTS (**Fig. 2a**, lane 3). The transfected MRPL18 undergoes less efficient processing than the endogenous counterpart, presumably owing to reduced mitochondrial import because the transgene lacks the 3′ untranslated region (3′ UTR) of MRPL18 (ref. 19). As expected, the imported exogenous MRPL18 incorporated into mitochondrial ribosomes, as evidenced by its cosedimentation with other mitoribosomal proteins (**Supplementary Fig. 1d**). Upon heat-shock stress, the full-length wild-type MRPL18 (MRPL18(WT)) showed a modest increase, whereas we observed much less change for MRPL18(ATG), which lacks both the 5′ UTR and the MTS region (**Fig. 2a**, lanes 9 and 10). Remarkably, the CUG-only MRPL18(C14A) exhibited the strongest responsiveness despite its low basal levels in cells without stress (**Fig. 2a**, lanes 7 and 8). To substantiate this finding further, we constructed reporters by replacing the main coding region of MRPL18 with firefly luciferase (Fluc). Consistently with the immunoblotting results of MRPL18 mutants, the chimeric C14A-Fluc exhibited the highest increase of Fluc expression in response to heat-shock stress (**Fig. 2b**).

Having confirmed the stress-induced alternative translation of MRPL18 by using mutants, we next sought to determine whether MRPL18(WT) undergoes a translational switch from the authentic AUG to the downstream CUG in response to heat-shock stress. It is challenging to unequivocally monitor the newly synthesized MRPL18(cyto) because of the high basal levels of MRPL18(mito) present in cells before stress. To circumvent this limitation, we engineered a reversible destabilization domain (DD) by fusing it to the COOH terminus of MRPL18(WT) (**Fig. 2c**). This system permits temporal examination of newly synthesized MRPL18-DD after addition of Shield-1, a cell-permeable drug that binds the DD to protect the protein from degradation[20]. HeLa cells transfected with plasmids expressing MRPL18-DD exhibited minimal anti-myc signals in the absence of Shield-1 (**Supplementary Fig. 2a**). Treatment with Shield-1 stabilized MRPL18-DD, which had a clear mitochondrial localization (**Fig. 2c** and **Supplementary Fig. 2b**). Remarkably, heat-shock stress before Shield-1 addition resulted in substantial anti-myc signals in the cytosol as well as the nucleus (**Fig. 2c** and **Supplementary Fig. 2c**). This observation was not due to mitochondrion leakage, because the stress-induced Hsp60 remained exclusively in mitochondria after heat shock. This result confirms that heat-shock stress triggers CUG-mediated alternative translation within the wild-type sequence context of MRPL18.

MRPL18(cyto) is dependent on eIF2α phosphorylation

What is the mechanism underlying stress-induced alternative translation of MRPL18? We looked into eukaryotic initiation factor 2α (eIF2α), whose phosphorylation regulates ATF4, in a classical example of alternative translation triggered by many stress conditions[21–24]. Consistently with a previous report[25], heat-shock stress also triggered eIF2α phosphorylation (**Supplementary Fig. 3a**). To address the role of eIF2α phosphorylation in the alternative translation of MRPL18, we transfected MRPL18-Fluc reporters into a mouse embryonic fibroblast (MEF) cell line bearing a nonphosphorylatable eIF2α in which

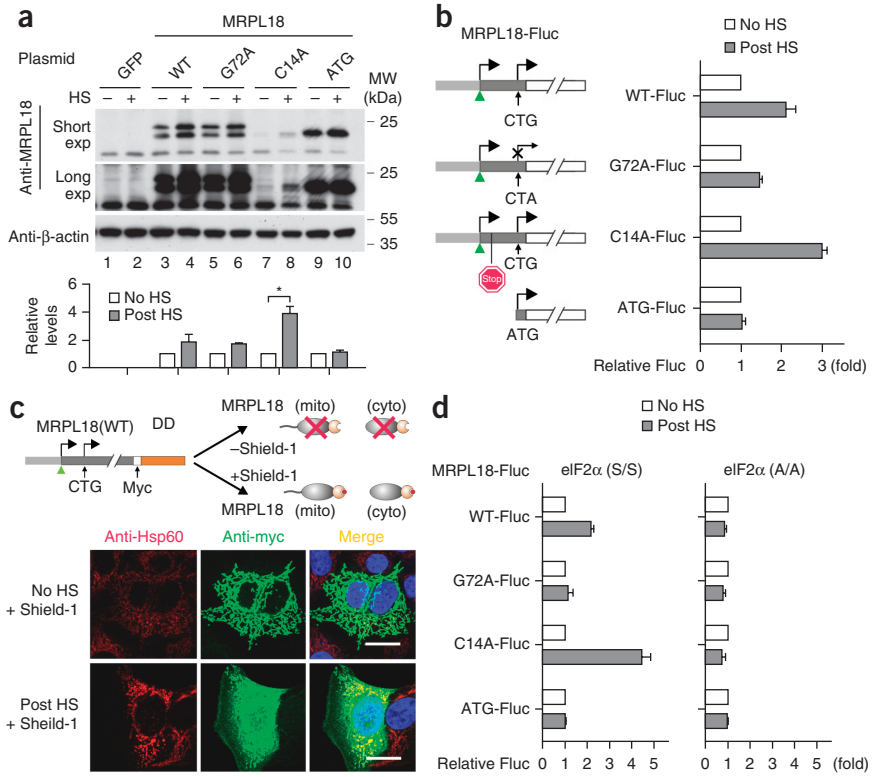

Figure 2 MRPL18 undergoes alternative translation in a stress-dependent manner. (**a**) Representative immunoblot results of HeLa cells transfected with the indicated plasmids and collected before heat shock (HS) or 2.5 h after heat shock (43 °C, 1 h). Top bands are uncleaved MRPL18 precursors. β-actin is a loading control. The bottom graph shows the relative levels of transgenes (small isoform) normalized to β-actin. Error bars, s.e.m. ($n = 3$ cell cultures, $^*P < 0.01$ by two-tailed Student's t test). MW, molecular weight; exp, exposure. (**b**) Fluc reporter assays in HeLa cells transfected with MRPL18-Fluc constructs shown at left. Fluc activities after heat shock are normalized to those in nonstressed cells. Error bars, s.e.m. ($n = 3$ cell cultures). (**c**) Immunostaining of HeLa cells transfected with MRPL18-DD with or without heat shock in the presence of Shield-1. Anti-Hsp60 antibody is shown in the red channel and anti-myc in the green channel. Scale bars, 10 μm. A schematic of MRPL18-DD fusion protein in the absence or presence of Shield-1 is shown at top. (**d**) Fluc reporter assays in eIF2α (S/S) and eIF2α (A/A) MEFs transfected with MRPL18-Fluc constructs shown in **b**. Fluc activities after heat shock are normalized to those of nonstressed cells. Error bars, s.e.m. ($n = 3$ cell cultures). Original blot images are in **Supplementary Data Set 1**.

Ser51 (S/S genotype) was mutated to an alanine (A/A genotype)[26]. As expected, wild-type MEF (S/S) cells showed a similar pattern of Fluc expression as HeLa cells (**Fig. 2d**). In particular, the CUG-only MRPL18(C14A) exhibited the highest increase of Fluc (more than four-fold) in response to heat-shock stress, whereas the expression level of the AUG-only MRPL18(G72A) remained unchanged. Remarkably, the stress responsiveness of MRPL18(C14A) was completely abolished in MEF (A/A) cells (**Fig. 2d** and **Supplementary Fig. 3b**), thus indicating that the alternative translation of MRPL18 is dependent on eIF2α phosphorylation.

MRPL18(cyto) integrates into cytosolic 80S ribosomes

Given that the authentic role of MRPL18 is to constitute the ribosome complex within mitochondria, we speculated that MRPL18(cyto) may integrate into the cytosolic 80S ribosome complex under stress conditions. To test this hypothesis, we assessed the behavior of endogenous MRPL18 as well as transfected mutants in HeLa cells. We first purified cytosolic ribosome complexes with affinity immunoprecipitation (IP) in order to eliminate mitochondrial ribosome contamination. We also converted the polysomes into monosomes by RNase I digestion before IP to exclude indirect pulldown of RNA-binding proteins (**Fig. 3a**). Endogenous MRPL18, but not other mitochondrial proteins, was readily precipitated from stressed cells by either anti-RPL4 or anti-RPS6 antibodies (**Fig. 3a**, lanes 2 and 6). In addition, we recovered endogenous MRPL18 from the polysome fraction after heat-shock stress and found that this redistribution was sensitive to the translation inhibitor cycloheximide (CHX) (**Supplementary Fig. 4**). Therefore, the cytosolic ribosome-associated MRPL18 is newly synthesized after

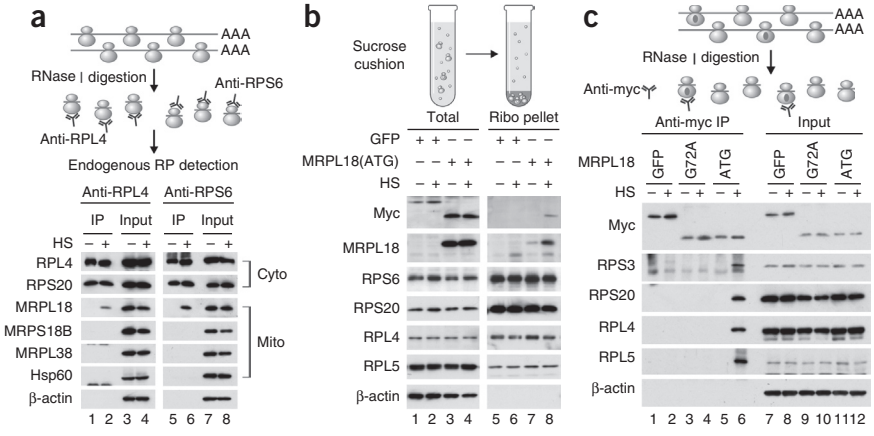

Figure 3 Cytosolic MRPL18 incorporates into the 80S ribosome in a stress-dependent manner. (**a**) Detection of MRPL18 in endogenous ribosomes purified from HeLa cells with or without heat shock. Immunoblotting of RNase I–digested cell lysates immunoprecipitated with anti-RPL4 (left) or anti-RPS6 (right) antibodies. Input and immunoprecipitates (IP) are indicated. Cyto, cytoplasmic; mito, mitochondrial. (**b**) Immunoblot detection of myc-tagged MRPL18(ATG) from endogenous ribosomes isolated by sucrose cushion from HeLa cells with or without heat shock. HeLa cells transfected with GFP are a control. Total lysate and ribosome (ribo) pellet are indicated. (**c**) Immunoblot detection of cytosolic ribosomal proteins from anti-myc immunoprecipitates. Samples are HeLa cells transfected with myc-tagged MRPL18(ATG), with or without heat shock, and HeLa cells transfected with GFP and MRPL18(G72A) as controls. Cell lysates were treated with RNase I before anti-myc IP. Throughout figure, β-actin is a loading control. Experiment schematics are shown at top. Original blot images are in **Supplementary Data Set 1**.

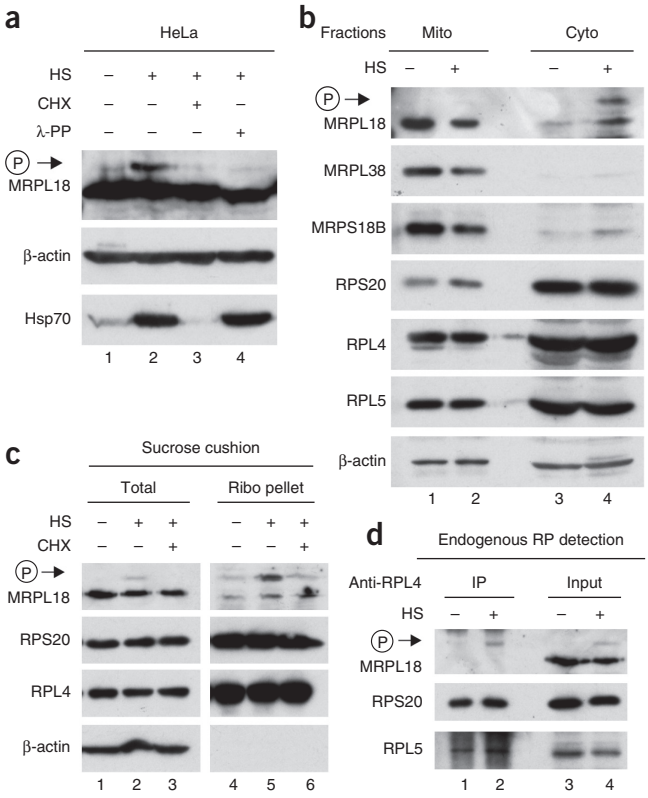

Figure 4 Cytosolic MRPL18 incorporates into the 80S ribosome in a phosphorylation-dependent manner. (**a**) Detection of phosphorylated MRPL18 in HeLa cells with or without heat-shock stress. Immunoblotting of whole cell lysates with or without λ-phosphatase (λ-PP) treatment, separated with Phos-tag acrylamide gel (MRPL18 only) or standard PAGE. CHX treatment during heat shock was included to demonstrate phosphorylation of newly synthesized MRPL18. (**b**) Detection of phosphorylated (P) MRPL18 in HeLa cell fractions with or without heat-shock stress. Immunoblotting of HeLa lysates with or without heat shock, fractionated with a mitochondria fractionation kit and separated with Phos-tag acrylamide gel (MRPL18 only) or standard PAGE. (**c**) Detection of phosphorylated MRPL18 in ribosome fractions of HeLa cells with or without heat-shock stress. Immunoblotting of total lysate and ribosome fractions prepared by sucrose cushion, separated with Phos-tag acrylamide gel (MRPL18 only) or standard PAGE. (**d**) Detection of phosphorylated MRPL18 in ribosomes purified from HeLa cells with or without heat-shock stress. Immunoblotting of RNase I–digested total lysates and anti-RPL4 immunoprecipitates, separated with Phos-tag acrylamide gel (MRPL18 only) or standard PAGE. Throughout figure, β-actin is a loading control. Original blot images are in **Supplementary Data Set 1**.

stress. We further confirmed the incorporation of MRPL18(cyto) into the 80S ribosome complex by using transfected MRPL18(ATG). Both cosedimentation binding analysis and anti-myc IP revealed a robust association of MRPL18(ATG) with cytosolic ribosomes in a stress-dependent manner (**Fig. 3b**, lane 8 and **Fig. 3c**, lane 6). In contrast, the AUG-only MRPL18(G72A) did not coprecipitate with any cytosolic RPs before or after heat-shock stress (**Fig. 3c**).

Phosphorylated MRPL18(cyto) integrates into 80S ribosomes

Interestingly, very little transfected MRPL18(ATG) was associated with the 80S ribosome in unstressed cells in spite of comparable expression levels. To investigate the mechanism of stress-induced incorporation, we examined the phosphorylation status of MRPL18 by using a Phos-tag acrylamide gel. An MRPL18 band with slower migration was clearly discernible upon heat-shock stress, and it was sensitive to phosphatase treatment (**Fig. 4a**). Addition of the translation inhibitor CHX completely abolished this species, thus suggesting that newly synthesized MRPL18 is phosphorylated during stress. Importantly, we found the phosphorylated MRPL18 exclusively in the cytosolic fraction (**Fig. 4b**), and we recovered only the phosphorylated species from the cytosolic 80S ribosome (**Fig. 4c**,**d**). We next searched for the kinase responsible for MRPL18 phosphorylation. Interestingly, MRPL18 was predicted to be a substrate of the tyrosine protein kinase Lyn[27]. Indeed, both the Lyn-specific chemical inhibitor bafetinib (**Fig. 5a**) and small hairpin RNA (shRNA)-mediated knockdown of Lyn (**Fig. 5b**) reduced the phosphorylation level of MRPL18. Notably, Lyn is a member of the Src family, whose kinase activity is increased upon heat-shock stress[28]. These results collectively indicate that both the production and function of MRPL18(cyto) are under tight control in response to stress.

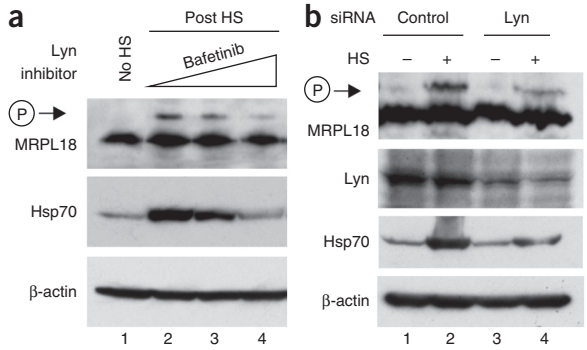

Figure 5 Cytosolic MRPL18 undergoes Lyn-mediated phosphorylation. (**a**) Detection of phosphorylated MRPL18 in HeLa cells in the presence of increasing doses of bafetinib immediately after heat-shock stress. Immunoblotting of whole cell lysates separated with Phos-tag acrylamide gel (MRPL18 only) or standard PAGE. (**b**) Detection of phosphorylated MRPL18 in HeLa cells transfected with SMARTpool siRNAs targeting Lyn or control shRNA targeting scrambled sequences. Immunoblotting of whole cell lysates separated with Phos-tag acrylamide gel (MRPL18 only) or standard PAGE. Throughout figure, β-actin is a loading control. Original blot images are in **Supplementary Data Set 1**.

MRPL18(cyto) promotes stress-protein synthesis during stress

The stress-inducible feature of MRPL18(cyto) is suggestive of its regulatory role in the cytosolic stress response. To elucidate its physiological function, we knocked down MRPL18 in HeLa cells with SMARTpool small interfering RNAs (siRNAs). Reduction in MRPL18 expression had minimal effects on cell growth and did not alter the rate of global protein synthesis (**Supplementary Fig. 5a**). In addition, we observed minimal effects of MRPL18 depletion on mitochondrial translation after short-term siRNA knockdown or long-term lentivirus-based shRNA knockdown (**Supplementary Fig. 5b**,**c**). However, upon heat-shock treatment, the induction of Hsp70 expression in the cytosol was largely dampened in cells with MRPL18 knockdown compared to cells transfected with control siRNA (**Fig. 6a**). To substantiate this finding further, we applied shRNA to HeLa cells and MEFs (**Fig. 6b** and **Supplementary Fig. 6**). shRNA-mediated MRPL18 knockdown resulted in impaired Hsp70 induction in both cells after heat-shock stress. This result was not due to transcriptional deficiency of Hsp70 gene expression. In fact, MEFs with MRPL18 knockdown demonstrated even higher Hsp70 transcript levels than the control cells in response to heat-shock stress (**Supplementary Fig. 6d**).

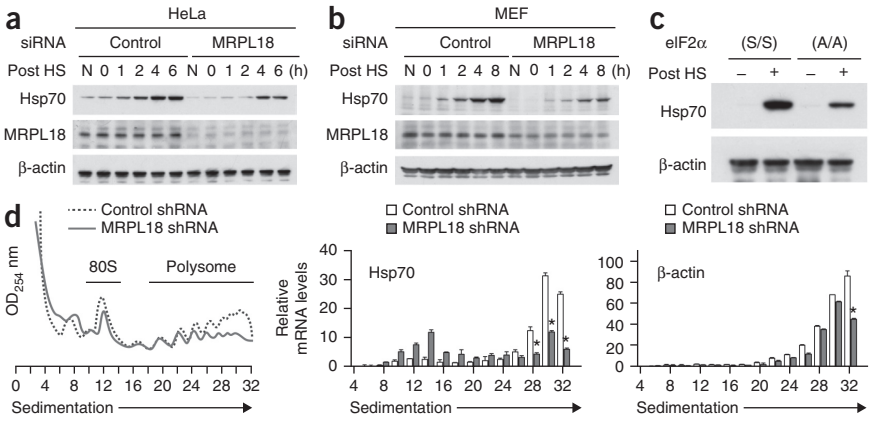

Figure 6 Cytosolic MRPL18 promotes Hsp70 biosynthesis after heat-shock stress. (**a**) Examination of heat shock–induced Hsp70 synthesis in HeLa cells transfected with SMARTpool siRNAs targeting MRPL18 or control shRNA targeting scrambled sequences. Immunoblotting of cell lysates collected at indicated times after heat shock. N, no heat shock. (**b**) Examination of heat shock–induced Hsp70 synthesis in MEFs infected with lentiviruses expressing shRNAs targeting MRPL18 or control shRNA. Immunoblotting of cell lysates collected at the indicated times after heat shock. (**c**) Examination of heat shock–induced Hsp70 synthesis in eIF2α (S/S) and eIF2α (A/A) MEFs after heat-shock stress. (**d**) Examination of polysome-enriched Hsp70 mRNA in MEFs infected with lentiviruses expressing shRNA targeting MRPL18 or control shRNA. Quantitative PCR measuring Hsp70 and β-actin mRNA levels in total RNA extracted from polysome fractions. Relative levels are normalized to the total. OD_{254}, optical density at 254 nm. Error bars, s.e.m. ($n = 3$ cell cultures, $^*P < 0.05$ by two-tailed Student's t test). Throughout figure, β-actin is a loading control. Original blot images are in **Supplementary Data Set 1**.

Given that the *de novo* synthesis of MRPL18(cyto) relies on alternative translation, we reasoned that suppressing CUG initiation would have a similar effect as MRPL18 knockdown. Indeed, stress-induced Hsp70 synthesis was substantially reduced in eIF2α (A/A) cells, whose eIF2α is not phosphorylatable (**Fig. 6c**). Because the incorporation of MRPL18(cyto) into the 80S ribosome is phosphorylation dependent, we examined the effects of reduced Lyn kinase activities in the stress response. Treatment with the Lyn inhibitor bafetinib or Lyn knockdown dramatically suppressed Hsp70 induction after heat-shock stress (**Fig. 5a**,**b**). The deficient Hsp70 synthesis is specific to MRPL18 because knocking down other mitochondrial ribosomal proteins did not influence the cytosolic stress response at all (**Supplementary Fig. 7a**,**b**). These data collectively highlight MRPL18(cyto) as a critical mediator of the cytosolic stress response.

MRPL18(cyto) promotes ribosome engagement on stress mRNAs

The participation of MRPL18(cyto) in Hsp70 synthesis suggests that a specialized ribosome might be required for mRNA translation under stress conditions. MRPL18 is a homolog of cytoplasmic RPL5, according to sequence alignment. Much like RPL5, MRPL18 binds to 5S rRNA and is believed to import the 5S rRNA into mitochondria[29]. An *in vitro* RNA binding assay confirmed that 5S rRNA strongly associates with recombinant MRPL18(ATG) but not GFP (**Supplementary Fig. 7d**,**e**). However, we found little evidence indicating that MRPL18 replaces RPL5 in binding to the 80S ribosome (**Fig. 3**). In fact, RPL5 knockdown also reduced Hsp70 synthesis after heat-shock stress (**Supplementary Fig. 7c**). Notably, MRPL18 does not seem to interact with separated 40S or 60S subunits (**Supplementary Fig. 7f**). It is thus likely that MRPL18(cyto) serves as an extra RP in binding to the

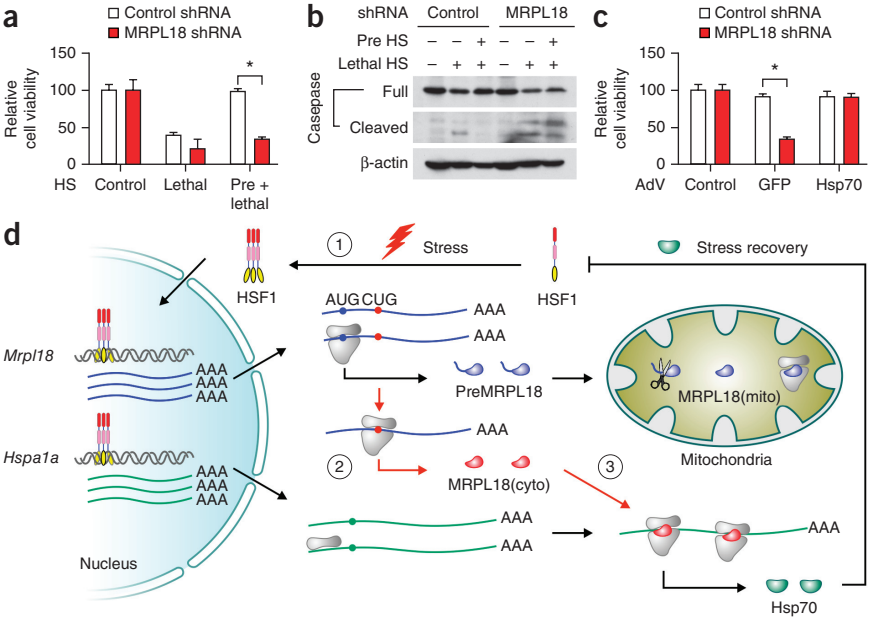

Figure 7 Cytosolic MRPL18 is essential for induced thermal tolerance. (**a**) Thermal tolerance analysis of MEFs lacking MRPL18. MEFs transfected with shRNA targeting MRPL18 or control shRNA targeting scrambled sequences were primed with mild heat shock (43 °C for 30 min) and allowed to recover at 37 °C for 5 h (pre). Severe heat shock (45 °C for 1 h; lethal) was then applied before the cell viability assay. Error bars, s.e.m. ($n = 4$ cell cultures, $^*P < 0.01$ by two-tailed Student's t test). Control, no heat shock. (**b**) Examination of apoptotic markers in MEF cells as in **a** by immunoblotting with the indicated antibodies. (**c**) Thermal tolerance assays of MEFs after reintroduction of Hsp70. MEFs as in **a** were infected with recombinant adenoviruses (AdV) encoding GFP or Hsp70 before thermal tolerance analysis. Error bars, s.e.m. ($n = 3$ cell cultures, $^*P < 0.01$ by two-tailed Student's t test). Control, uninfected cells. (**d**) A model for MRPL18 in translational control during stress conditions. Stress conditions such as heat shock trigger trimerization and activation of HSF1 (1), which turns on genes including *Mrpl18* and *Hspa1a*. In nonstressed cells, MRPL18 translation is initiated from the annotated AUG, generating MRPL18 containing a mitochondria localization signal (blue). In stressed cells, MRPL18 undergoes alternative translation from the downstream CUG start codon, which results in a cytoplasmic isoform of MRPL18 (red) (2). MRPL18(cyto) incorporates into the 80S ribosome complex, facilitating the engagement of mRNAs highly expressed under stress, such as *Hspa1a* (green) (3). The efficient synthesis of heat-shock proteins contributes to stress recovery. Original blot images are in **Supplementary Data Set 1**.

80S ribosome. 5S rRNA forms the central protuberance of the large ribosomal subunit[30]. This region is of particular importance because it nears the place where the ribosomal large and small subunits, the decoded mRNA and the peptidyl tRNA all come together. We postulate that the presence of an extra RP promotes 80S ribosome engagement on mRNAs during stress conditions. To test this hypothesis, we examined the distribution of Hsp70 mRNA in the polysome fractions of stressed MEF cells with or without MRPL18 knockdown (**Fig. 6d**). With comparable total mRNA levels, the Hsp70 transcript showed much less enrichment in the polysomes of MEFs lacking MRPL18. In contrast, control β-actin mRNA exhibited only minor reduction in the polysomes of these cells, presumably because of the delayed stress recovery as a result of impaired Hsp70 synthesis. Indeed, MEFs lacking MRPL18 showed less polysome formation during stress recovery (**Fig. 6d**).

MRPL18 is essential for induced thermotolerance

Because of the essential role of chaperone molecules in cell survival, we predict that cells lacking MRPL18 should have attenuated thermotolerance. Induced thermotolerance allows cells to survive a normally lethal temperature if they are first conditioned at a milder temperature. Without preconditioning, MEFs with or without MRPL18 knockdown were equally susceptible to severe heat stress at 45 °C for 1 h (**Fig. 7a**). Preexposure at 43 °C for 30 min resulted in a nearly complete protection of control MEF cells from severe heat stress. However, we no longer observed the induced thermotolerance in MEFs with MRPL18 knockdown. As expected, the reduced cell viability in the absence of MRPL18 was largely due to increased apoptosis (**Fig. 7b**). In agreement with the suppressed chaperone biosynthesis in cells lacking MRPL18, reintroduction of Hsp70 by recombinant adenoviruses completely restored the thermotolerance (**Fig. 7c**). Given the broad range of chaperone function in cell physiology, it would be of much interest to investigate possible protective roles of MRPL18 against cellular stressors beyond heat shock.

DISCUSSION

Cells in nearly all living organisms respond to heat-shock stress by marked transcriptional alterations and rapid translational reprogramming[5]. Despite severe inhibition of the translation machinery under stress conditions, efficient synthesis of stress proteins persists by a mechanism that has not been completely understood. Here, we uncovered a molecular mechanism underlying the active translation of mRNAs highly expressed during stress. We show that heat-shock stress triggers a previously unrecognized alternative translation of MRPL18, which generates a cytoplasmic isoform of the mitochondrial ribosomal protein. Remarkably, the cytoplasmic version of MRPL18 incorporates into the 80S ribosome complex in a stress-dependent manner. The stress-induced formation of specialized ribosomes, together with the cap-independent translation initiation mechanism, ensures efficient translation of mRNAs under nonfavorable conditions (**Fig. 7d**). Our results thus provide a new paradigm for translational regulation under stress conditions, which involves ribosome specialization after an initial alternative translation event.

A growing body of evidence has suggested that ribosome heterogeneity prevails across species, under different developmental stages and in various tissues[31,32]. Variation in ribosome composition, in both rRNA and RPs, provides a regulatory mechanism to the translation machinery. A clear example is illustrated in *Escherichia coli*, in which the stress-induced endonuclease MazF cleaves the 16S rRNA and removes the anti–Shine-Dalgarno sequence[33]. The resultant 'stress ribosome' selectively translates the leaderless mRNAs, a group of transcripts also generated by MazF. In eukaryotes, certain RPs have been found to control transcript selectivity during translation. For example, RPL38 is required for translation of homeobox mRNAs[34], whereas RPL40 appears to control translation of vesicular stomatitis virus mRNAs[35]. In this report, we discovered in mammalian cells an unusual mechanism that allows HSP mRNA translation to escape from the shutoff of global protein synthesis. Instead of altering the rRNA structure, the mammalian stress ribosome uses an extra RP that functions in mitochondria at basal state. MRPL18(cyto) incorporation may alter ribosome conformation and/or stabilize ribosome engagement on mRNAs that are highly expressed under stress conditions. Alternatively, the presence of MRPL18(cyto) may cause recruitment of additional factors facilitating initiation and elongation. In any case, stress-induced ribosome heterogeneity permits translational reprogramming without rebuilding the entire translational machinery.

Another interesting phenomenon revealed by our data is the functional connection between mitochondrial and cytoplasmic ribosomes. The 55S mitochondrial ribosome differs substantially from the 80S ribosome in eukaryotic cytoplasm and the 70S ribosome in prokaryotes. In mammalian cells, the mitochondrial ribosome complex has a higher content of protein than rRNA components[14,36]. Although many MRPs are distinctive and evolving rapidly, MRPL18 has a close homolog in *E. coli*. Unlike many other RPs, MRPL18 has apparently evolved to become a stress-inducible gene in mammals. The possession of an alternative translation feature further renders MRPL18 a critical regulator of the stress response. We conclude that MRPL18 actively participates in stress adaptation by potentiating the cellular translation machinery to achieve a robust cytosolic stress response.

METHODS

Methods and any associated references are available in the online version of the paper.

Note: Any Supplementary Information and Source Data files are available in the online version of the paper.

ACKNOWLEDGMENTS

We thank J.W. Yewdell and T. Fox for critical reading of the manuscript. We also thank I. Benjamin (University of Utah) for providing *Hsf1*$^{+/+}$ and *Hsf1*$^{-/-}$ MEFs, R. Kaufman (Sanford Burnham Medical Research Institute) for eIF2α (S/S) and eIF2α (A/A) MEFs, and T. Wandless (Stanford) for plasmids encoding the FKBP destabilizing domain. This work was supported in part by US National Institutes of Health training grants to R.A.C. and C.S.C. B.L. was supported as a recipient of the Genomics Scholar's Award from the Center for Vertebrate Genomics at Cornell. This work was primarily supported by grants to S.-B.Q. from the US National Institutes of Health (DP2 OD006449 and R01AG042400), the Ellison Medical Foundation (AG-NS-0605-09) and the US Department of Defense (W81XWH-14-1-0068).

AUTHOR CONTRIBUTIONS

X.Z. and S.-B.Q. conceived the original idea and designed the experiments. X.Z. performed the majority of the experiments. X.G. conducted luciferase reporter assays. R.A.C. assisted in polysome gradient analysis. C.S.C. conducted ^{35}S metabolic labeling assays. B.L. assisted in data interpretation. S.-B.Q. wrote the manuscript, and all authors edited the manuscript.

COMPETING FINANCIAL INTERESTS

The authors declare no competing financial interests.

1. Holcik, M. & Sonenberg, N. Translational control in stress and apoptosis. *Nat. Rev. Mol. Cell Biol.* **6**, 318–327 (2005).
2. Spriggs, K.A., Bushell, M. & Willis, A.E. Translational regulation of gene expression during conditions of cell stress. *Mol. Cell* **40**, 228–237 (2010).
3. Jackson, R.J., Hellen, C.U. & Pestova, T.V. The mechanism of eukaryotic translation initiation and principles of its regulation. *Nat. Rev. Mol. Cell Biol.* **11**, 113–127 (2010).

4. Panniers, R. Translational control during heat shock. *Biochimie* **76**, 737–747 (1994).
5. Richter, K., Haslbeck, M. & Buchner, J. The heat shock response: life on the verge of death. *Mol. Cell* **40**, 253–266 (2010).
6. Morimoto, R.I. Regulation of the heat shock transcriptional response: cross talk between a family of heat shock factors, molecular chaperones, and negative regulators. *Genes Dev.* **12**, 3788–3796 (1998).
7. Anckar, J. & Sistonen, L. Regulation of HSF1 function in the heat stress response: implications in aging and disease. *Annu. Rev. Biochem.* **80**, 1089–1115 (2011).
8. McGarry, T.J. & Lindquist, S. The preferential translation of *Drosophila* hsp70 mRNA requires sequences in the untranslated leader. *Cell* **42**, 903–911 (1985).
9. Klemenz, R., Hultmark, D. & Gehring, W.J. Selective translation of heat shock mRNA in *Drosophila melanogaster* depends on sequence information in the leader. *EMBO J.* **4**, 2053–2060 (1985).
10. Rubtsova, M.P. *et al.* Distinctive properties of the 5′-untranslated region of human hsp70 mRNA. *J. Biol. Chem.* **278**, 22350–22356 (2003).
11. Sun, J., Conn, C.S., Han, Y., Yeung, V. & Qian, S.B. PI3K-mTORC1 attenuates stress response by inhibiting cap-independent Hsp70 translation. *J. Biol. Chem.* **286**, 6791–6800 (2011).
12. Moore, P.B. How should we think about the ribosome? *Annu Rev Biophys* **41**, 1–19 (2012).
13. Kressler, D., Hurt, E. & Bassler, J. Driving ribosome assembly. *Biochim. Biophys. Acta* **1803**, 673–683 (2010).
14. Christian, B.E. & Spremulli, L.L. Mechanism of protein biosynthesis in mammalian mitochondria. *Biochim. Biophys. Acta* **1819**, 1035–1054 (2012).
15. Lee, S., Liu, B., Huang, S.X., Shen, B. & Qian, S.B. Global mapping of translation initiation sites in mammalian cells at single-nucleotide resolution. *Proc. Natl. Acad. Sci. USA* **109**, E2424–E2432 (2012).
16. Trinklein, N.D., Murray, J.I., Hartman, S.J., Botstein, D. & Myers, R.M. The role of heat shock transcription factor 1 in the genome-wide regulation of the mammalian heat shock response. *Mol. Biol. Cell* **15**, 1254–1261 (2004).
17. Mendillo, M.L. *et al.* HSF1 drives a transcriptional program distinct from heat shock to support highly malignant human cancers. *Cell* **150**, 549–562 (2012).
18. Qian, S.B., McDonough, H., Boellmann, F., Cyr, D.M. & Patterson, C. CHIP-mediated stress recovery by sequential ubiquitination of substrates and Hsp70. *Nature* **440**, 551–555 (2006).
19. Margeot, A. *et al.* In *Saccharomyces cerevisiae*, ATP2 mRNA sorting to the vicinity of mitochondria is essential for respiratory function. *EMBO J.* **21**, 6893–6904 (2002).
20. Banaszynski, L.A., Chen, L.C., Maynard-Smith, L.A., Ooi, A.G. & Wandless, T.J. A rapid, reversible, and tunable method to regulate protein function in living cells using synthetic small molecules. *Cell* **126**, 995–1004 (2006).
21. Sonenberg, N. & Hinnebusch, A.G. New modes of translational control in development, behavior, and disease. *Mol. Cell* **28**, 721–729 (2007).
22. Harding, H.P., Calfon, M., Urano, F., Novoa, I. & Ron, D. Transcriptional and translational control in the mammalian unfolded protein response. *Annu. Rev. Cell Dev. Biol.* **18**, 575–599 (2002).
23. Vattem, K.M. & Wek, R.C. Reinitiation involving upstream ORFs regulates ATF4 mRNA translation in mammalian cells. *Proc. Natl. Acad. Sci. USA* **101**, 11269–11274 (2004).
24. Wek, R.C., Jiang, H.Y. & Anthony, T.G. Coping with stress: eIF2 kinases and translational control. *Biochem. Soc. Trans.* **34**, 7–11 (2006).
25. Duncan, R.F. & Hershey, J.W. Protein synthesis and protein phosphorylation during heat stress, recovery, and adaptation. *J. Cell Biol.* **109**, 1467–1481 (1989).
26. Scheuner, D. *et al.* Translational control is required for the unfolded protein response and *in vivo* glucose homeostasis. *Mol. Cell* **7**, 1165–1176 (2001).
27. Yamanashi, Y. *et al.* The yes-related cellular gene lyn encodes a possible tyrosine kinase similar to p56lck. *Mol. Cell. Biol.* **7**, 237–243 (1987).
28. Lin, R.Z., Hu, Z.W., Chin, J.H. & Hoffman, B.B. Heat shock activates c-Src tyrosine kinases and phosphatidylinositol 3-kinase in NIH3T3 fibroblasts. *J. Biol. Chem.* **272**, 31196–31202 (1997).
29. Smirnov, A., Entelis, N., Martin, R.P. & Tarassov, I. Biological significance of 5S rRNA import into human mitochondria: role of ribosomal protein MRP-L18. *Genes Dev.* **25**, 1289–1305 (2011).
30. Szymański, M., Barciszewska, M.Z., Erdmann, V.A. & Barciszewski, J. 5 S rRNA: structure and interactions. *Biochem. J.* **371**, 641–651 (2003).
31. Xue, S. & Barna, M. Specialized ribosomes: a new frontier in gene regulation and organismal biology. *Nat. Rev. Mol. Cell Biol.* **13**, 355–369 (2012).
32. Gilbert, W.V. Functional specialization of ribosomes? *Trends Biochem. Sci.* **36**, 127–132 (2011).
33. Vesper, O. *et al.* Selective translation of leaderless mRNAs by specialized ribosomes generated by MazF in *Escherichia coli*. *Cell* **147**, 147–157 (2011).
34. Kondrashov, N. *et al.* Ribosome-mediated specificity in Hox mRNA translation and vertebrate tissue patterning. *Cell* **145**, 383–397 (2011).
35. Lee, A.S., Burdeinick-Kerr, R. & Whelan, S.P. A ribosome-specialized translation initiation pathway is required for cap-dependent translation of vesicular stomatitis virus mRNAs. *Proc. Natl. Acad. Sci. USA* **110**, 324–329 (2013).
36. O'Brien, T.W. Properties of human mitochondrial ribosomes. *IUBMB Life* **55**, 505–513 (2003).

ONLINE METHODS

Cell lines and reagents. HeLa cells were maintained in Dulbecco's Modified Eagle's Medium (DMEM) with 10% FBS. *Hsf1*$^{+/+}$ and *Hsf1*$^{-/-}$ MEFs were kindly provided by I.J. Benjamin (University of Utah). Cycloheximide (CHX), poly(U) and puromycin were purchased from Sigma. MitoTracker (M-7512), Mitochondria-GFP (C10508), Alexa Fluor 488– or Alexa Fluor 546–labeled secondary antibodies (donkey anti-mouse IgG (H+L) (A21202 and A10036)) and Hoechst (H1399) were purchased from Invitrogen. Anti-MRPL18 (HPA028774), anti-MRPL38 (HPA023054), anti-RPS20 (HPA003570), anti-RPL5 (HPA043717), anti-myc (C3956) and anti–β-actin (A5441) monoclonal antibody were purchased from Sigma; anti-MRPS18B (16139-1-AP) and anti-RPL4 (11302-1-AP) were from Proteintech; anti-Hsp70 (SPA810) was from Enzo Life Sciences; and anti-RPS6 (2217), anti-HSP60 (4870), anti-Caspase 3 (9662) and cleaved Caspase 3 (9661) antibodies were from Cell Signaling. Validation is provided on the manufacturers' websites. The Dual luciferase kit was purchased from Promega. SMARTpool siRNAs targeting human MRPL18 and control were purchased from Dharmacon. siRNAs targeting human Lyn, MRPL38 and MRPS18B were purchased from Santa Cruz Biotechnology. Plasmids and siRNA transfections were performed with Lipofectamine 2000 (Invitrogen) according to the manufacturer's instructions.

Plasmids. MRPL18 cDNA was cloned from total RNAs extracted from HeLa cells by RT-PCR. The amplified MRPL18 cDNA contains both the 5′ UTR and the coding sequence, and it was inserted into pcDNA3.1/myc-his (Invitrogen). For MRPL18 mutants, mutagenesis was performed with the QuikChange II site-directed mutagenesis kit according to the manufacturer's instructions (Stratagene). For MRPL18-Fluc constructs, an *Eco*RI site downstream of the CTG codon was used to replace the MRPL18 with firefly luciferase (Fluc) derived from pGL3 (Promega). For MRPL18-DD constructs, the FKBP destabilization domain (DD) was amplified from pBMN and subcloned into pcDNA3.1/ MRPL18. All plasmids were confirmed by DNA sequencing.

Lentiviral shRNAs. All shRNA targeting sequences were cloned into DECIPHER pRSI9-U6-(sh)-UbiC-TagRFP-2A-Puro (Cellecta). shRNA targeting sequences were from the RNAi consortium at the Broad Institute (http://www.broadinstitute.org/rnai/trc/). MRPL18(human), 5′ CTCAGAGAATCTATGAATAAA 3′; MRPL18(mouse), 5′ CCAAAGGAAAGCATC TGCATT 3′; control sequence, 5′ AACAGTCGCGTTTGCGACTGG 3′. Lentiviral particles were packaged with Lenti-X 293T cells (Clontech). Virus-containing supernatants were collected at 48 h after transfection and were filtered to eliminate cells, and target cells were infected in the presence of 8 μg ml^{-1} polybrene. 24 h later, cells were selected with 5 μg ml^{-1} puromycin.

Immunoprecipitation. Cells were washed twice with PBS and lysed in ice-cold lysis buffer (20 mM HEPES, pH 7.4, 150 mM NaCl, 5 mM $MgCl_2$, 0.5 mM DTT, 1× EDTA-free complete protease inhibitor (Roche), 100 μg ml^{-1} CHX, and 20 μg ml^{-1} Poly(U)) supplemented with 1% NP-40. Cell lysates were incubated on ice for 1 h and then were treated with 2 μl RNase I (Ambion) for another 1 h at 4 °C. Lysates were spun at 20,000*g* for 10 min at 4 °C, and supernatants were collected and then incubated with anti-myc agarose beads (Sigma) at 4 °C overnight. Immunoprecipitates were washed four times with gradient buffer (10 mM HEPES, pH 7.4, 150 mM NaCl, and 5 mM $MgCl_2$) containing 1% NP-40. The washed beads were resuspended in 1× SDS sample buffer (100 mM Tris, pH 6.8, 2% SDS, 15% glycerol, 5% β-mercaptoethanol, and 0.1% bromophenol blue), boiled for 10 min, and analyzed by immunoblotting.

Immunoblotting. Cells were lysed on ice in TBS buffer (50 mM Tris, pH 7.5, 150 mM NaCl, and 1 mM EDTA) containing protease inhibitor–cocktail tablet, 1% Triton X-100, and 2 U ml^{-1} DNase. After incubation on ice for 30 min, the lysates were heated for 10 min in SDS-PAGE sample buffer (50 mM Tris, pH 6.8, 100 mM dithiothreitol, 2% SDS, 0.1% bromophenol blue, and 10% glycerol). Proteins were resolved on SDS-PAGE and were transferred to Immobilon-P membranes (Millipore). For Phos-tag SDS-PAGE, 50 μM Phos-tag acrylamide (Wako) and 50 μM $MnCl_2$ (Sigma) were added to 12% acrylamide gel, and electrophoresis was performed in a manner identical to standard SDS-PAGE. After electrophoresis, Mn^{2+} was removed from the Phos-tag gel by incubation with 1× transfer buffer containing 1 mM EDTA for 10 min. EDTA was then removed by incubation with 1× transfer buffer for another 10 min before the transfer. Membranes were blocked for 1 h in TBS containing 5% BSA, and this was followed by incubation with primary antibodies. After incubation with horseradish peroxidase–coupled secondary antibodies (Sigma A9917 and A9169), immunoblots were developed with enhanced chemiluminescence (ECL^{Plus}, GE Healthcare).

***In vitro* RNA synthesis and binding assay.** Full-length human 5S and 5.8S rRNA were amplified with a forward primer carrying a T7 polymerase target sequence (underlined) and a reverse primer: 5S rRNA forward, 5′-TAATACG ACTCACTATAGGGGTCTACGGCCATACCACC CTG-3′; 5S rRNA reverse, 5′-AAAGCCTACAGCACCCGGTAT-3′; 5.8S rRNA forward, 5′-TAATAC GACTCACTATAGGG GACTCTTAGCGGTGGATC-3′; 5.8S rRNA reverse, 5′-AAGCGACGCTCAGACAGGC-3′.

Purified PCR product was used as a template for *in vitro* transcription. *In vitro* transcription was carried out with the MEGAshortscript kit (Ambion) according to the manufacturer's instructions. The coding sequence of MRPL18 without the mitochondrial target sequence (MRPL18(ATG)) was subcloned into the pET-30a vector. *E. coli* strain BL21(DE3) was used as the host for protein expression, and proteins were purified by Ni-NTA agarose (Qiagen). Binding of MRPL18(ATG) to 5S rRNAs was measured by a shift in the mobility of the RNA in 1.8% agarose gels run at room temperature at 100 V. Binding reactions were performed in buffer containing 20 mM HEPES, pH 8.0, 30 mM NH_4Cl, 100 mM KCl, 0.5 mM $MgCl_2$, 1 mM DTT, 4% glycerol, 0.1% Nonidet P-40, acetylated bovine serum albumin (0.05 mg/ml), and RNase inhibitor (0.2 units/ml of RNase OUT (Invitrogen)). Protein and RNA at the indicated concentrations were mixed gently and incubated at room temperature for 30 min. After addition of Hi-Density TBE Sample Buffer (Invitrogen), the reactions were loaded onto a 1.8% agarose gel and electrophoresed in TAE buffer (40 mM Tris acetate and 1 mM EDTA) at 100 V for 30 min. After electrophoresis, the RNA was visualized by ethidium bromide staining.

Polysome profiling analysis. Polysome buffer (10 mM HEPES, pH 7.4, 100 mM KCl, 5 mM $MgCl_2$, 100 μg ml^{-1} cycloheximide and 2% Triton X-100) was used to prepare sucrose solutions. Sucrose density gradients (15–45% (w/v)) were freshly made in SW41 ultracentrifuge tubes (Beckman) with a Gradient Master (BioComp Instruments) according to the manufacturer's instructions. Cells were pretreated with 100 μg ml^{-1} cycloheximide for 3 min at 37 °C to stabilize ribosomes on mRNAs; this was followed by washing with ice-cold PBS containing 100 μg ml^{-1} cycloheximide. Cells were then lysed by extensive scraping in polysome lysis buffer. Cell debris was removed by centrifugation at14,000 r.p.m. for 10 min at 4 °C. 600 μl of supernatant was loaded onto sucrose gradients; this was followed by centrifugation for 100 min at 38,000 r.p.m. at 4 °C in a SW41 rotor. Separated samples were fractionated at 0.750 ml/min through an automated fractionation system (Isco) that continually monitors OD_{254} values. Fractions were collected at 0.5-min intervals. Aliquots of the ribosome fraction were used to extract total RNA with TRIzol LS reagent (Invitrogen) for real-time PCR analysis or were heated at 98 °C for 10 min in SDS sample buffer (50 mM Tris-HCl, pH 6.8, 100 mM dithiothreitol, 2% SDS, 0.1% bromophenol blue, and 10% glycerol) for western blot analysis.

For polysome concentration, fractions corresponding to more than two ribosomes were pooled and diluted 1:1 with gradient buffer. Polysomes were pelleted by centrifugation for 2 h at 4 °C at 300,000*g* in polycarbonate centrifuge tubes (Beckman 349622) in a TLA110 rotor (Beckman) with a tabletop ultracentrifuge (Optima MAX, Beckman). Polysome pellets were resuspended in 1× SDS sample buffer for western blot analysis.

Ribosome sucrose cushion. Ribosome sucrose cushion analyses were conducted with a previously described protocol with minor modifications[37]. In brief, HeLa cells were collected in lysis buffer (20 mM Tris, pH 7.4, 10 mM $MgCl_2$, 300 mM KCl, 10 mM dithiothreitol, 100 units/ ml RNase OUT, 20 μg ml^{-1} Poly(U) and 100 μg ml^{-1} cycloheximide). Cell lysates were incubated on ice for 1 h and then were centrifuged at 12,500*g* for 10 min to remove mitochondria and debris. The supernatant was layered over 1 ml of a 1 M sucrose cushion; this was followed by centrifugation at 60,000 r.p.m. for 2 h in a Beckman TLA-110 rotor. The ribosome-containing pellet was rinsed twice with 200 μl ice-cold water and resuspended in 1× SDS sample buffer for western blot analysis.

RNA isolation and PCR. Total cellular RNA was extracted with TRIzol reagent (Invitrogen) according to the manufacturer's instructions. Contaminating DNA was digested by pretreatment with RNase-free DNase (Ambion). Single-strand cDNA synthesis was carried out with the High-Capacity cDNA Reverse Transcription kit (Applied Biosystems); this was followed by standard PCR reactions. Real-time PCR reactions were performed with Power SYBR Green Mater Mix (Applied Biosystems) with a LightCycler 480 Real-time PCR System (Roche). Gene expression was normalized to β-actin cDNA levels and calculated as a relative gene expression with the $2^{-\Delta\Delta Ct}$ method.

Oligonucleotide primers are as follows: human MRPL18, forward 5′-CATCAG AATGGCAAGGTTGTG-3′ and reverse 5′-AAGTTGATTCCCGCCTCTAAG-3′; mouse MRPL18, forward 5′-AGCAAAGGAAGATAGGGCAC-3′ and reverse 5′-ACA GACATTTCCAGAACCGC-3′; human HSPA1A, forward 5′-TGTG TAACCCCATCA TCAGC-3′ and reverse 5′-TCTTGGAAAGGCCCCTAATC-3′; mouse HSPA1A, forward 5′-TGGTGCAGTCCGACATGAAG-3′ and reverse 5′-GCTGAGAGTCGTTG AAGTAGGC-3′; human β-actin, forward 5′-AGCC TCGCCTTTGCCGA-3′ and reverse 5′-GCGCGGCGATATCATCATC-3′; mouse β-actin, forward 5′-TTGCTGACAGGA TGCAGAAG-3′ and reverse 5′-ACTCCTGCTTGCTGATCCACAT-3′. Quantitation of target genes of each fraction was normalized with the reference firefly luciferase. Primers used are forward 5′-ATCCGGAAGCGACCAACGCC-3′ and reverse 5′-GTCG GGA AGACCTGCCACGC-3′.

^{35}S metabolic labeling. Cells were washed with DPBS (pH 7.0, Invitrogen) before incubation in methionine-free DMEM (Invitrogen) for 15 min at 37 °C. After quick centrifugation, cells were resuspended in labeling media (methionine-free DMEM supplemented with 10% FBS and 10 μCi ml^{-1} [^{35}S] mix (PerkinElmer)). At the indicated time points, aliquots were transferred to ice-cold stop buffer (DMEM supplemented with 1 mg ml^{-1} L-methionine, 1 mg ml^{-1} L-cysteine and 100 μg ml^{-1} cycloheximide). Cells were centrifuged at 12,500 r.p.m. for 5 min, and the cell pellets were washed with ice-cold DPBS supplemented with 1 mg ml^{-1} of L-methionine and L-cysteine with 100 μg ml^{-1} cycloheximide. The washed cell pellets were lysed in ice-cold lysis buffer (10 mM HEPES, pH 7.4, 100 mM KCl, 5 mM $MgCl_2$, 100 μg ml^{-1} cycloheximide and 2% Triton X-100) for 30 min; this was followed by centrifugation at 12,500 r.p.m. at 4 °C for 10 min. The supernatant was collected and precipitated with 10% trichloroacetic acid (Sigma). The mixture was heated for 10 min at 90 °C; this was followed by a 10-min incubation on ice. The precipitates were collected on GF/C filter membranes (Whatman) and then washed with 10% TCA and 100% ethanol. The dried membrane was measured for ^{35}S incorporation with scintillation counting (Beckman Coulter).

For mitochondria translation, cells were pretreated with 100 μg ml^{-1} cycloheximide for 5 min before 1 h metabolic labeling in labeling medium supplemented with 100 μg ml^{-1} cycloheximide in the absence or presence of 100 μg ml^{-1} chloramphenicol. Whole cell lysates were separated on a 12% SDS-PAGE gel, which was then subjected to autoradiography.

Luciferase assay. Real-time measurements of Fluc activity were recorded at 37 °C with 5% CO_2 with a KronosDio Luminometer (Atto) as previously described[11]. In brief, cells were plated on 35-mm dishes and transfected with plasmids encoding Fluc. 12 h after transfection, cells were subjected to heat shock (43 °C, 1 h), and 1 mM luciferase substrate D-luciferin (Regis Tech) was added into the culture medium. For Hsp70-Fluc experiments, cells were subjected to heat shock 1 h after transfection; this was followed by the addition of 1 mM luciferase substrate D-luciferin.

Immunofluorescence staining. Cells grown on glass coverslips were fixed in 4% paraformaldehyde and permeabilized by 0.2% Triton X-100. After being blocked in 2% BSA in PBS, fixed cells were incubated with the primary antibody at 4 °C overnight; this was followed by a 1-h incubation at room temperature with Alexa Fluor–labeled secondary antibodies (Invitrogen A21202 and A10036). Cells were then washed with PBS and incubated for 5 min in PBS supplemented with Hoechst to counterstain the nuclei. After a final wash of cells with PBS, cover slips were mounted onto slides and viewed with a confocal microscope (Zeiss LSM710).

Cell viability assay. MEFs infected with lentiviruses expressing shRNA targeting MRPL18 or control shRNA were selected for stable expression. For induction of heat-shock response, cells were incubated in a 43 °C water bath for 30 min and allowed to recover at 37 °C for 5 h (pre HS). Lethal heat stress (45 °C for 1 h) was subsequently applied, and cells were then incubated at 37 °C for 24 h. Cells were then used for viability assay with the Cell Counting Kit-8 (Dojindo Molecular Technologies) or were collected for western blot analysis. For rescue assays, 24 h before lethal heat stress, cells were infected with recombinant adenoviruses encoding GFP or Hsp70 at ~10 MOI before viability assays were performed.

37. Mazumder, B. *et al.* Regulated release of L13a from the 60S ribosomal subunit as a mechanism of transcript-specific translational control. *Cell* **115**, 187–198 (2003).

doi:10.1038/nsmb.3010